Title

Mussel-Inspired Conductive Polymer Binder for Si-Alloy Anode in Lithium-Ion Batteries

Journal

ACS Applied Materials & Interfaces, 10(6)

ISSN

1944-8244

Authors

Zhao, Hui

Wei, Yang

Wang, Cheng

et al.

Publication Date

2018-02-14

DOI

10.1021/acsami.7b14645

Peer reviewed

Mussel-inspired conductive polymer binder for Si-alloy anode in lithium-ion batteries

Hui Zhao,[a]† Yang Wei,[b,c]† Cheng Wang,[d] Ruimin Qiao,[d] Wanli Yang,[d] Phillip B. Messersmith,[b,e*] and Gao Liu[a*]

[a]*Energy Storage and Distributed Resources Division, Energy Technologies Area,* [d]*Advanced Light Source, and* [e]*Materials Sciences Division, Lawrence Berkeley National Laboratory, Berkeley, California, 94720, United States*

[b]*Department of Materials Science and Engineering, UC Berkeley, California, 94720, United States*

[c]*Department of Chemical Engineering and Biotechnology, National Taipei University of Technology, Taipei, Taiwan*

† These authors contributed equally to this work

Keywords: mussel-inspired, conductive polymer binder, silicon anode, lithium-ion battery, single molecule detection

Abstract: The excessive volume changes during cell cycling of Si-based anode in lithium ion batteries impeded its application. One major reason for the cell failure is particle isolation during volume shrinkage in delithiation process, which makes strong adhesion between polymer binder and anode active material particles a highly desirable property. Here, a biomimetic side-chain conductive polymer incorporating catechol, a key adhesive component of the mussel holdfast protein, was synthesized. Atomic force microscopy (AFM) based single molecule force measurements of mussel-inspired conductive polymer binder contacting a silica surface revealed similar adhesion toward substrate when compared with an effective Si anode binder, homo-polyacrylic acid (PAA), with the added benefit of being electronically conductive.

Electrochemical experiments showed very stable cycling of Si-alloy anodes realized via this biomimetic conducting polymer binder, leading to a high loading Si anode with good rate performance. We attribute the ability of the Si-based anode to tolerate volume changes during cycling to the excellent mechanical integrity afforded by the strong interfacial adhesion of the biomimetic conducting polymer.

Introduction

The lithium-ion battery (LIB) has enabled revolutionary changes in the development of portable computers, cell phones, digital cameras, long-driving-range electric vehicles and the storage of renewable energy in utility power grids. High-capacity active materials and components are key to the next generation of high-energy LIB. The most popular graphite anode only has a gravimetric specific capacity of 372 mAh/g, while alternative alloy anode materials such as tin (Sn, 994 mAh/g) or silicon (Si, 4200 mAh/g) have much higher gravimetric specific capacities.[1] However, almost 300% volume expansion occurs as the material transitions from Si to its fully lithiated $Li_{15}Si_4$ phase.[2] Because of this large volume change as well as continuous adverse surface side reactions, the electronic integrity of the composite electrode is disrupted during cycling, leading to a drastic decay in battery capacity.[3] The electrode laminate should adhere uniformly onto the current collector, as active Si particles need good adhesion to the current collector and cohesion in the laminate to ensure the flow of ions and electrons.

Polymeric binders have shown their unique role in addressing this problem, as good interfacial adhesion among Si particles is a prerequisite to endure the drastic volume changes in the Si-based system. Incorporating hydrogen bonding elements into a low T_g polymer binder enables self-healing of the electrode crack and satisfactory cycling performance of a Si

micro-particle based anode.[4] For example, cross-linked binder systems incorporating dual carboxylic acid and hydroxyl groups was shown to effectively accommodate the large volume change during cycling, resulting in good cycling stability.[5,6] These previous works demonstrate the modification of binder as a viable path to drive the application of high-capacity Si-based anodes.[7,8]

In spite of several novel concepts in polymer binder,[9] further improvements in polymer binder properties are needed. An intrinsically-conductive polymer binder can eliminate the use of acetylene black conductive additives to simply the electrode design, provide electronically conductivity to the entire surface of the active materials particles rather than point contacts with acetylene black conductive additives, and maintain the integrity of the anode during cycling due to stronger adhesions. Some of successful improvements have been developed based upon this idea. A backbone-conjugated polyfluorene-type conductive polymer enabled a long-term cycling of Si and SiO anode.[7,10] A side chain-conjugating pyrene polymer proved to be a good binder for Si-based anode, while allowing easy optimization of the polymer structure.[8,11] Wu *et al.* designed a conducting hydrogel by in-situ polymerization to conformally coat silicon nanoparticles, which led to a long-term stable cycling.[12]

In addition to intrinsic conductivity, improvements for stronger interfacial adhesion in polymer binder properties are also required. Numerous material developments are inspired by the observation and investigation of phenomena in the natural world.[13] With respect to interfacial adhesion, mussels rely on byssal threads to attach to underwater surfaces. Long-lasting adhesion in their wet environment is due at least in part to the catecholic amino acid 3,4-dihydroxy-L-phenylalanine (DOPA) in the specialized adhesive proteins.[14,15] Inspection of mussel adhesive protein offers insight into the rational design of mussel-mimetic polymeric

binders for Si-based lithium-ion batteries.[16] In the present work, we synthesized a copolymer consisting of conducting and catecholic building blocks, quantitatively studied the molecular interfacial adhesion, and studied the electrochemical performance of a Si-alloy anode made from the conductive polymer binder. Both cases require adhesion in liquid, as the byssal threads attach to water wetted surfaces and catecholic binder adhesive attaches to the electrolyte wetted Si surface. Results of this work demonstrate the impressive stable cycling performance achieved by the dual strategy of mussel-inspired adhesion and conductive polymer.

Results and Discussion

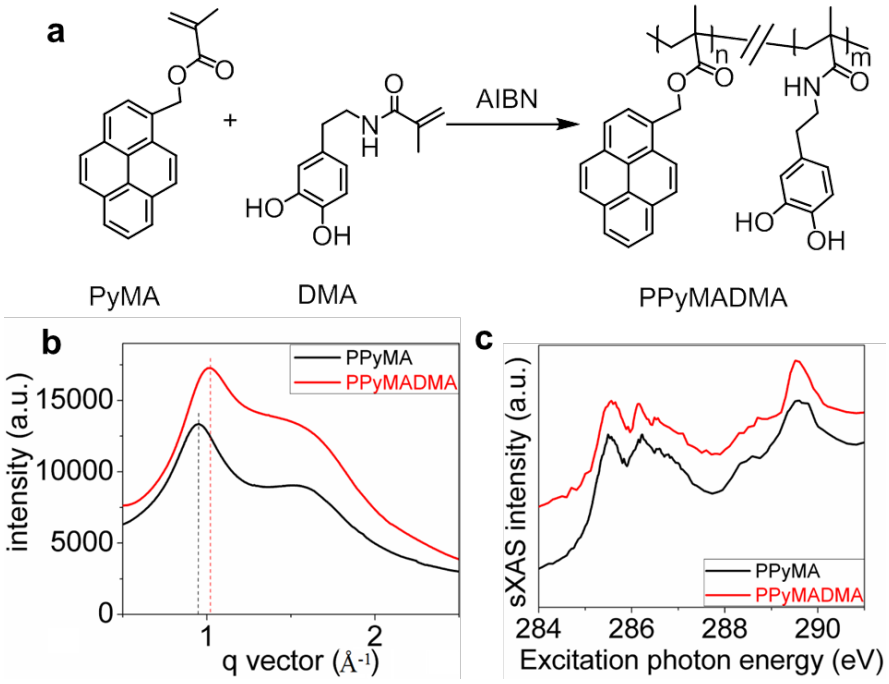

Figure 1. (a) Generic synthesis of poly(1-pyrenemethyl methacrylate-*co*-dopamine methacrylamide) (PPyMADMA). (b) Wide angle X-ray scattering (WAXS) of PPyMA and PPyMADMA polymers. (c) Carbon K-edge sXAS of PPyMA and PPyMADMA shows that the LUMO energy is intact in PPyMADMA, although non-conductive DMA groups are introduced.

Mussel-Inspired Polymer binder. Pyrene (Py)-based polymers derived from 1-pyrenemethyl methacrylate (PyMA) were established as candidate electrically-conducting polymers. The flexible chain backbone of these polymers allows self-assembly of the Py side chains into ordered structures, realizing electron conductivity via the side chain π-π stacking force of the aromatic Py

moieties.[17,18] A versatile radical-based polymerization was used to synthesize PPyMA and also facilitated the incorporation of additional functional groups. For adhesion, we used the building block of dopamine methacrylamide (DMA) synthesized based on a literature procedure.[16] Poly(1-pyrenemethyl methacrylate-*co*-dopamine methacrylamide) (PPyMADMA) was synthesized through free-radical polymerization where the adhesive monomer, DMA, accounts for 36 mol% of this copolymer (^{1}H- nuclear magnetic resonance spectroscopy) (Figure 1a). PPyMADMA had a number-average molecular weight of 29,000 Dalton and a polydispersity index of 1.9, while being soluble in solvents such as tetrahydrofuran (THF) and N-methylpyrrolidone (NMP). The data for PPyMA in Figure 1b and 1c were shown in our previous publication,[11] and are incorporated here for comparison. Wide-angle X-ray scattering (WAXS) results show the ordered phase characteristic of the pyrene in both PPyMA and PPyMADMA (Figure 1b). Diffraction peaks are located at ~0.95 $Å^{-1}$ and ~1.02 $Å^{-1}$, respectively. This corresponds to a lattice spacing of ~0.6 nanometers (nm). The broadening of the diffraction peak for the PPyMADMA sample indicates that the crystal grain size is smaller when copolymerized with DMA (Figure 1b).

To ensure that the newly-designed PPyMADMA binder still maintains the electronic conductivity, we studied the electronic structure of both the PPyMA and PPyMADMA polymers using synchrotron-based x-ray absorption spectroscopy (sXAS). sXAS is a direct probe of the excitations of core level electrons to the unoccupied valence states. Previous results demonstrate that sXAS is the tool-of-choice to reveal the critical electron state associated with the electric properties of polymer binder materials in batteries.[7,10] The methodology is based on the principle that the lowest-energy sXAS feature directly corresponds to the state of the lowest unoccupied

molecular orbital (LUMO), which defines the electric properties of the polymers.[19] We also note that a comparative sXAS measurement between polymers with different functional groups is reliable without the core-hole potential concerns.[7] Figure 1c shows such a comparison of the sXAS spectra of PPyMA and PPyMADMA. The splitting peaks around 285-286 eV correspond to the $\pi^*_{C=C}$ bonds with conjugation, and the features around 288 eV are from $\pi^*_{C=O}$.[19] Focusing on the low-energy sXAS features corresponding to the LUMO states, it is obvious that incorporating the DMA group does not change the lowest-energy features in sXAS, indicating the LUMO of the PPyMA polymer is intact in PPyMADMA. Except for a finite change at high energies away from the LUMO states, the consistency of the overall lineshape implies that the electron states close to the Fermi level are dominated by the pyrene-based PPyMA states.

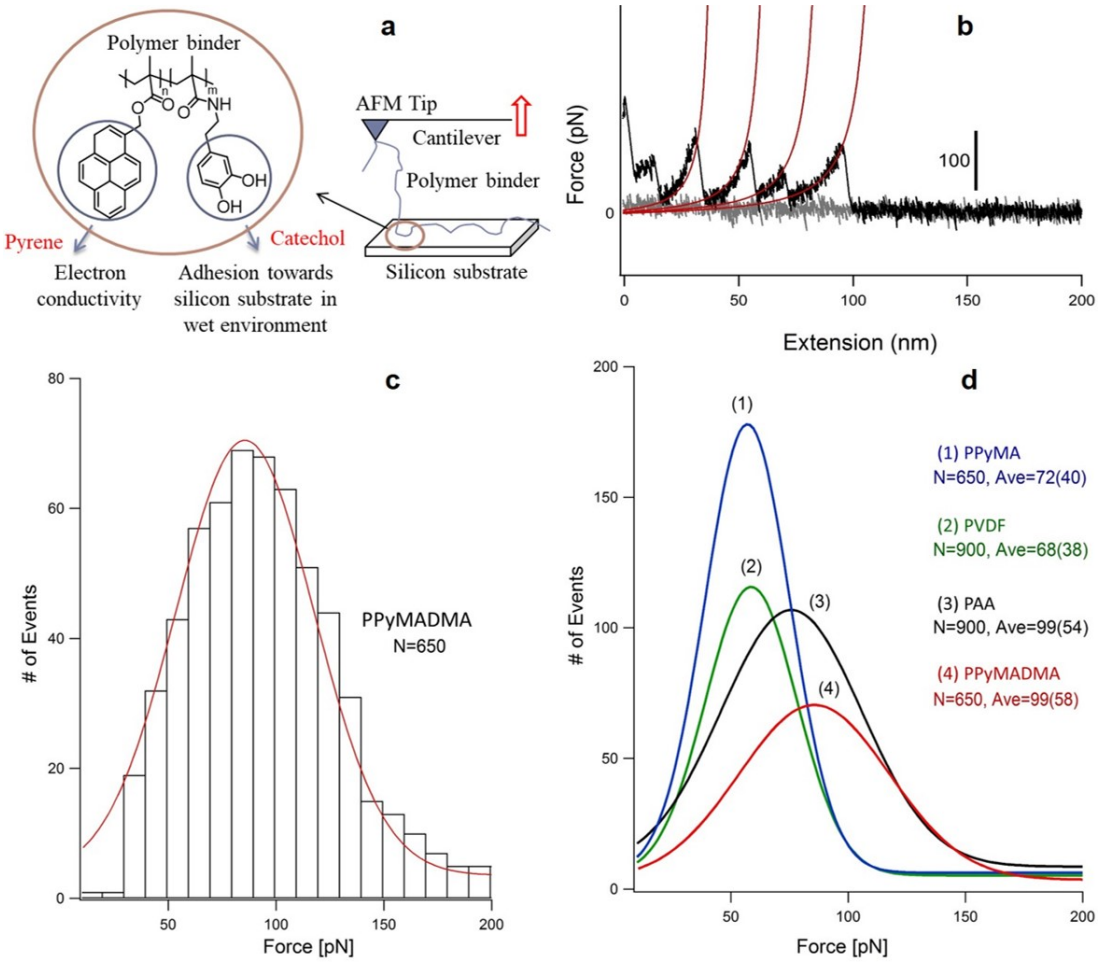

Figure 2. (a) A schematic drawing of the unbinding force measurement using an AFM, which involves pulling a PPyMADMA polymer binder from silicon substrate with both of the cathchol-based adhesive mechanism and pyrene-based conductive domains involved. (b)Representative raw AFM force-extension curves representing pulling PPyMADMA polymer binder from glass surface in 1M LiCl, pH 6.7. The successful worm-like chain model fits to the force curve are shown in red. Details regarding curve fitting are described in Figure S7 in supporting information. (c) Histograms of AFM rupture force distribution corresponding to pulling a single PPyMADMA polymer chain from a glass surface. Gaussian fit to the experimental data is shown in red. (d) Gaussian fits of AFM rupture force distribution adopted from figure 2b (i.e., PPyMADMA) and our previous research (i.e., PAA, PVDF and PPyMA)[11] corresponding to pulling a single chain of each polymer binders on glass substrate in 1M LiCl (pH 6.7), with the averaged rupture forces shown as 99±59, 99±54, 68±38 and 72±40 piconewton (pN), respectively (Ave=mean rupture force ± (standard deviations) and N= # of observed unbinding events). The pulling velocity is 1000 nm/s and dwell time is 0.5 seconds.

Molecular unbinding force of polymer binder from a silica substrate. The high volume changes of the Si-based anode during cell cycling may cause particle polymer delamination during delithiation/shrinkage of the anode particles, which is one of the major electrode failure mechanisms for these high-capacity anodes.[9] To characterize the binding affinity between polymer

binders and the Si-alloy anode particles, we investigated the unbinding forces originating from pulling a single PPyMADMA chain from glass substrate at a constant speed. We performed these experiments in a 1M LiCl electrolyte (pH=6.7) as an approximation of the electrolyte in a LIB. To ensure that the observed events originated from a single molecular unbinding event, we employed a screening protocol developed previously[11] for rejecting the unbinding force arising from multiple chains (details regarding this protocol are described in Figure S7 in supporting information). A schematic description regarding the adhesive mechanism along with conductive domains in our polymer binder design is shown in Figure 2a, with its typical AFM force-extension curve for a single chain unbinding event shown in Figure 2b along with successful fits to the data using the worm-like chain (WLC) model of polymer elasticity. This experiment was performed many times to generate a histogram of unbinding force as shown in Figure 2c. For the sake of comparison, the Gaussian fit of the histogram in Figure 2c is shown together in Figure 2d with previously published results[11] obtained from unbinding of conventional polymer binders PPyMA, PVDF, and poly(acrylic acid) (PAA) from glass substrate. With the understanding that higher unbinding force of a single polymer chain correlates to stronger affinity to the substrate, these data show a shift in the distribution to higher unbinding force for PAA and PPyMADMA when compared to PVDF and PPyMA. Raw data of AFM force-extension curves of a single chain unbinding event for the case of PPyMA, PVDF and PAA can be found in Figure S8 in supporting information and in our previous publication.[11]

Traditionally, nonconducting conventional synthetic polymer binders such as polyacrylic acid (PAA) are considered effective for Si anode binding due to the benefit of hydrogen bonding with the substrate.[5] On the other hand, conventional polymer binders such as PVDF are comparatively

poor Si anode binders due to the fact that this type of polymer interacts with the substrate merely through van der Waals forces.[20] As shown in Figure 2d, the narrow shape and average rupture force of PPyMA (blue line) and PVDF (green line) distributions are similar. On the other hand, the broader shape and higher average rupture force observed for the case of PPyMADMA (red line) and PAA (black line) suggest that our polymer binder design has similar affinity toward the glass substrate compared to other effective Si anode binder. Thus, based upon our sXAS and AFM force results combining PyMA and DMA building blocks within the same copolymer binder may produce both high conductivity and satisfactory adhesion.

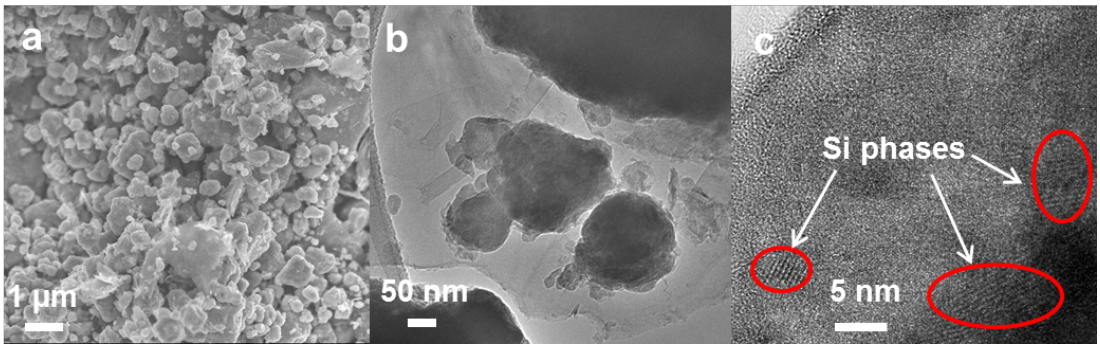

Figure 3. (a) SEM and (b) (c) High resolution TEM (HRTEM) of the Si alloy pristine particle.

Si-alloy anode. A Si-alloy is used as an anode to evaluate the electrochemical performance of the PPyMADMA polymer as a binder. The pristine particles have a diameter of typically around 1 μm (Figure 3a, 3b). Alloying the active Si elements with inactive elements can reduce volume expansion and yield an improved cycle life while still maintaining a specific capacity much higher than the graphite anode.[21] Si is present in nano-size domains (Figure 3c) within a matrix of other elements, such as Al and Fe. Not only is the volume expansion of the active Si phase buffered by the matrix, but the existence of the nano-Si domain could also suppress the formation of the crystalline $Li_{15}Si_4$.[22] A typical specific capacity of 800~1000 mAh/g is expected for this anode,

resulting in 100% volume change during cycling. Although this volume expansion is smaller than that of the pure Si materials, the absolute volume expansion of each particle is much larger than that of the 100 nm sized Si particles. Therefore stronger adhesion is needed to adhere the micron sized Si alloys together during charge and discharge process. This new PPyMADMA is designed to have much stronger adhesion than that of our conductive polymer binders reported earlier. The high gravimetric specific capacity of Si alloy can significantly reduce the active materials weight areal loading to ~0.5mg/cm^2, but still achieve the desired >3 mAh/cm^2 capacity loading for high energy density batteries.

PPyMADMA/Si alloy electrode performance. The dual functionality of intrinsic electronic conductivity and strong adhesion property of the PPyMADMA polymer makes it a promising binder in the use of Si-based high-capacity anode. The electrode was fabricated by dissolving PPyMADMA polymer into *N*-methylpyrrolidone (NMP), active material particles are then dispersed into the polymer solution by high-speed homogenizer for 1 hour before coating the slurry onto a Cu current collector using doctor blade. The PPyMADMA is not soluble in the common Li-ion electrolytes. Based on our extensive testing on different types of anode materials, PPyMADMA is a good binder for both graphite (Figure S2) and pure Si nanoparticles (Figure S1), without any need for conductive additives. In the conventional electrode design, the acetylene black conductive additive is required for enhancing the interfacial conductivity of the active materials. However, the functional conductive polymer binder provides superb adhesion to the surface of the active materials and electronic conductivities simultaneously. Conductive additive is not needed in our system, simplifying the electrode design. The good cycling performance shown in Figures S1 and S2 on Si and graphite indicate that by randomly incorporating catechol structure

into the polymer backbone, pyrene moieties still form good π-π stacking, enabling a good electric conductivity of the polymer binder and cycling performance of active materials.

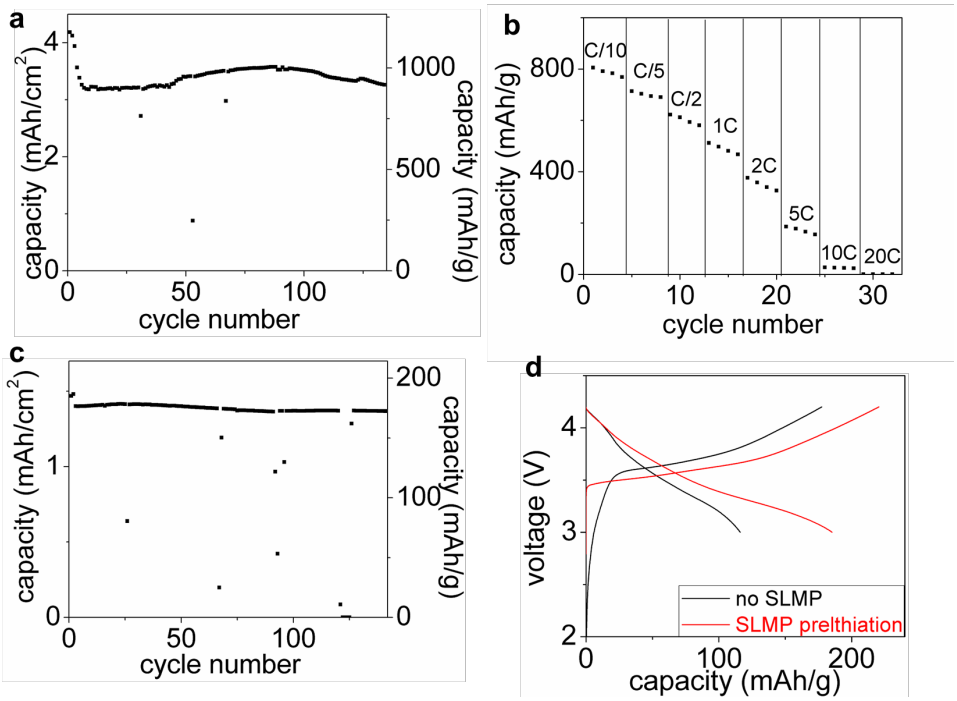

Figure 4. Electrochemical performance of PPyMADMA/Si alloy anode. (a) Areal capacity and specific capacity vs. cycle number of the PPyMADMA/Si alloy anode at C/10 in a half cell configuration. (b) Rate performance of the PPyMADMA/Si alloy anode in a half cell configuration. (c) Full cell cycling performance (Note, right axis label of capacity is based on NMC cathode material loading). (d) First cycle voltage curves using PPyMADMA/Si alloy anode, with or without stabilized lithium metal powder (SLMP®) prelithiation.

When used for the Si alloy anode, as shown in Figure 4a and Figure S5, 10 wt% PPyMADMA content is determined to be the best composition, maintaining a stable cycling of the Si alloy anode for more than 100 cycles with a specific capacity of 800 mAh/g. Compared to conventional binders such as polyvinylediene difluoride (PVDF) and carboxymethyl cellulose (CMC), which are intrinsically non-conductive, PPyMADMA exhibits an obvious advantage (Figure S6). A PPyMA homopolymer was also synthesized and used as a binder in a control experiment. Although PPyMA is an established conductive polymer binder for Si-based anode, PPyMA does not provide good adhesion strength between the binder and the Si alloy particles,

thus the PPyMA/Si-alloy electrode still suffers capacity decay. The rate performance of the PPyMADMA/Si alloy anode is shown in Figure 4b. Without any conductive additives, the specific capacity enabled by only PPyMADMA binder could still retain a specific capacity of above 500 mAh/g at 1C.

		10%PPyMADMA	5%PPyMADMA	10%CMC
1st cycle	Q_c[a](mAh/g)	845.2	1006.9	918.6
	H[b] (%)	64.64	77.95	82.69
10th cycle	Q_c[a] (mAh/g)	780.2	710.1	686.4
	H[b] (%)	99.38	98.27	97.86
70th cycle	Q_c[a] (mAh/g)	741.1	439.7	94.6
	H[b] (%)	99.85	99.20	98.22

[a] charge (delithiation) capacity [b] Coulombic efficiency

Table 1. Electrochemical data of the Si alloy anode based on different binders at C/10.

Table 1 summarizes the electrochemical results of Si alloy with different binders at a C/10 rate. The excellent capacity retention based on 10 wt% PPyMADMA binder is directly correlated to the good coulombic efficiency (CE) of the cell, which has a high value of 99.85% at 70th cycle, compared to 98.22% for the CMC binder. Note that the typical 1st CEs for the Si alloy is in the range of 70%, and a prelithiation method should be able to address issue toward a lithium-ion full cell application, which was demonstrated recently in a SiO anode.[23] Therefore, a nickel-cobalt-manganese (NCM 6/2/2) cathode was used to assemble full cell for the PPyMADMA/Si alloy anode and a 48-hour rest period allowed the crushed stabilized lithium metal powder (SLMP) to fully prelithiate the Si alloy anode before current-driven charging of the cells. Both full cells were put in a formation process consisting of two cycles at C/10 prior to C/3 cycling. Apparent improvement was shown for the SLMP-loaded full cells. The first cycle CE

increased from 65.41% to ~84% with the SLMP. The first cycle voltage curves of the full cells are shown in Figure 4d. Compared to the regular cell without SLMP, the voltage profile at both ends (start of charge and end of discharge) are distinctly different, indicating different lithiation and delithiation of Si alloy anode during these two stages. In the first cycle charge process, SLMP eliminated the needs for solid electrolyte interphase (SEI) formation and activation of the anode, so the curve goes directly to the anode lithiation voltage region. When SLMP is not used, the charging curve shows a long multi-plateau curvature accounting for a capacity of ~30 mAh/g, which is typical for irreversible processes of Si alloy anode activation and SEI formation.

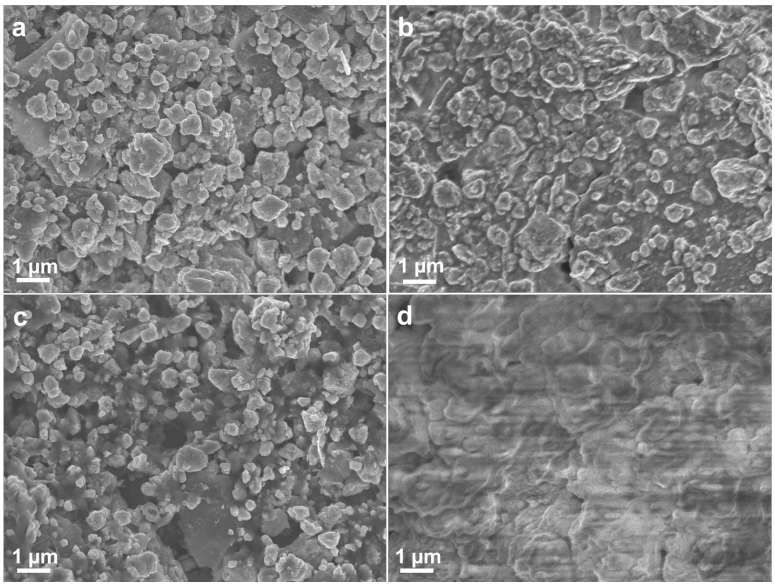

Figure 5. SEM images of the Si-alloy anode-based electrodes. (a) pristine and (b) after 10 cycles at C/10 of the PPy-DMA-based electrode. (c) pristine and (d) after 10 cycles at C/10 of the PVDF-based electrode.

Morphologies of the Si alloy electrodes. The SEM images of the Si electrodes before and after 10 cycles are shown in Figure 5. The most morphological changes of the Si electrode are in the first few cycles due to the large side reactions at the beginning. The cycling capacity of Si alloy electrode with a PVDF binder fades to almost zero in only a few cycles. Both electrodes based on PPyMADMA and PVDF binder appear similar before cycling tests. However, after cycling the

PVDF based electrode has large amount of surface residues from the SEI reactions, and the electrode is much more resistive as shown from the excessive charging during the SEM imaging process. Compared to the Si alloy electrode with a PVDF binder, the decomposition layer on the PPyMADMA-based electrode was much thinner. The Si alloy particles were still individually visible after 10 cycles of deep charge and discharge. In a conventional electrode with PVDF binder, the continuous volume change of active material particles makes the stable SEI formation impossible. The volume expansion of Si alloy during lithiation exposes new surfaces, leading to additional SEI formation and more side reaction products. However during delithiation, the Si particles shrink, and the SEI crumbles from the Si surface. These processes cause the formation of a thick layer of organic species due to the continuous decomposition of the electrolyte (Figure 5d). In contrast, the PPyMADMA conductive binder-based electrode has a much thinner SEI layer after repeated cycles, and SEI growth is very minimal. The edges of Si alloy particles are clearly visible with very minimum size changes after 10 cycles (Figure 5b). The PPyMADMA-based electrode has 10% binder to entirely cover the Si alloy particle surfaces. Due to the electric conductivity of the pyrene and the strong adhesion force of the catechol moiety, the intimate binding between binder and Si alloy particle is consistently maintained during cell cycling. The strong adhesion between PPyMADMA and Si-alloy particles ensures that the particle surface is completely covered by the binder to form an artificial SEI. The real SEI is formed on the surface of the PPyMADMA binder instead of on the active material particle surface directly. Since the polymer tends to have higher free volume, the PPyMADMA binder provides volume stability during Si volume expansion and contraction. PPyMADMA polymers completely cover the particle surface during the volume change, which reduces the contact between the Si alloy

particles and the electrolyte, and the continuous consumption of the electrolyte is hindered. Therefore, the SEI on the PPyMADMA/Si alloy electrode is much more stable compared to the SEI on the conventional composite. This is also confirmed by the high coulombic efficiency of 99.8% during long-term cycling. Based on our findings, the PPyMADMA copolymer could be considered an effective Si anode binder due to its ability to enhance interfacial adhesion while maintaining better electronic structure for *in situ* doping in the lithium ion battery anode operational voltage.

Conclusions

Integrating chemical moieties inspired by the mussel holdfast foot protein and established side-chain conducting groups, the DOPA-containing conductive copolymer PPyMADMA was shown to be an effective binder for a Si-alloy anode in lithium-ion batteries. The facile synthetic route of the side-chain conductive polymer relaxes the requirement for synthesis and allows easy incorporation of the functional adhesion moieties such as DOPA. A quantitative analysis of the adhesion between polymer and silica confirms the strong adhesion force, which contributed significantly to improving the capacity and cycle life of the Si alloy anode. The commercial Si-alloy anodes reach a high specific capacity of 800 mAh/g, a much higher value compared to the state-of-the-art graphite anode. When combined with a prelithiation method, the lithium ion full cell based on this novel binder-enabled high capacity anode delivers high 1st cycle efficiency (84%) and stable cycling at high material loadings. The mussel-inspired functional conductive polymer binder solves the volume expansion and low first-cycle coulombic efficiency problems, leading to a high-energy lithium-ion chemistry.

Supporting Information

Experimental procedures for synthesis of new polymer binder and its characterization data.

Experimental procedures including a screen protocol to collect the rupture force events when pulling single polymer binder from a substrate using an AFM tip.

This material is available free of charge via the Internet at http://pubs.acs.org.

Corresponding Author

* Tel.: +1-510-643-9631; Email: philm@berkeley.edu (P. Messersmith)
* Tel.: +1-510-486-7207; fax: +1-510-486-7303; Email: gliu@lbl.gov (G. Liu)

Author contributions

H.Z., Y.W., P.B.W. and G.L. conceived and designed the experiments. H.Z. and Y.W. performed the experiments. YC.W. performed the X-ray scattering characterization. R.Q. and W.Y. performed the X-ray absorption spectroscopy. G.L. and P.B.M. directed the project. All authors discussed and analyzed the data. H.Z., Y.W., P.B.M. and G.L. wrote the manuscript. † These authors contributed equally to this work

Competing financial interests

The authors declare no competing financial interests.

Acknowledgements

G. L. acknowledges funding support from the Assistant Secretary for Energy Efficiency, Vehicle Technologies Office of the U.S. Department of Energy (U.S. DOE) under the Advanced Battery Materials Research (BMR) and Applied Battery Research (ABR) Programs. Advanced Light Source (ALS), the Molecular Foundry, and the National Center for Electron Microscopy facilities are supported by the Director, Office of Science, Office of Basic Energy Sciences, of the U.S. Department of Energy, under Contract # DE-AC02-05 CH11231. Ruimin Qiao is supported by the LDRD program at the Lawrence Berkeley National Laboratory. The authors acknowledge partial support from NIH grant R37 DE014193.

References

1. *Boukamp, B. A.; Lesh, G. C.; Huggins, R. A., All-Solid Lithium Electrodes with Mixed-Conductor Matrix. Journal of The Electrochemical Society* ***1981,*** *128 (4), 725-729.*
2. *Li, J.; Dahn, J. R., An In Situ X-Ray Diffraction Study of the Reaction of Li with Crystalline Si. Journal of The Electrochemical Society* ***2007,*** *154 (3), A156-A161.*
3. *Ryu, J. H.; Kim, J. W.; Sung, Y.-E.; Oh, S. M., Failure Modes of Silicon Powder Negative*

Electrode in Lithium Secondary Batteries. Electrochemical and Solid-State Letters ***2004,*** *7 (10), A306-A309.*

4. *Wang, C.; Wu, H.; Chen, Z.; McDowell, M. T.; Cui, Y.; Bao, Z., Self-healing chemistry enables the stable operation of silicon microparticle anodes for high-energy lithium-ion batteries. Nat Chem* ***2013,*** *5 (12), 1042-1048.*
5. *Song, J.; Zhou, M.; Yi, R.; Xu, T.; Gordin, M. L.; Tang, D.; Yu, Z.; Regula, M.; Wang, D., Interpenetrated Gel Polymer Binder for High-Performance Silicon Anodes in Lithium-ion Batteries. Advanced Functional Materials* ***2014,*** *24 (37), 5904-5910.*
6. *Ling, M.; Zhao, H.; Xiaoc, X.; Shi, F.; Wu, M.; Qiu, J.; Li, S.; Song, X.; Liu, G.; Zhang, S., Low cost and environmentally benign crack-blocking structures for long life and high power Si electrodes in lithium ion batteries. Journal of Materials Chemistry A* ***2015,*** *3 (5), 2036-2042.*
7. *Liu, G.; Xun, S. D.; Vukmirovic, N.; Song, X. Y.; Olalde-Velasco, P.; Zheng, H. H.; Battaglia, V. S.; Wang, L. W.; Yang, W. L., Polymers with tailored electronic structure for high capacity lithium battery electrodes. Advanced Materials* ***2011,*** *23 (40), 4679-4683.*
8. *Park, S.-J.; Zhao, H.; Ai, G.; Wang, C.; Song, X.; Yuca, N.; Battaglia, V. S.; Liu, G., Side Chain Conducting and Phase-Separated Polymeric Binders for High-Performance Silicon Anodes in Lithium-Ion Batteries. Journal of the American Chemical Society* ***2015,*** *137 (7), 2565-2571.*
9. *Zhao, H.; Yuan, W.; Liu, G., Hierarchical electrode design of high-capacity alloy nanomaterials for lithium-ion batteries. Nano Today* ***2015,*** *10.*
10. *Wu, M.; Xiao, X.; Vukmirovic, N.; Xun, S.; Das, P. K.; Song, X.; Olalde-Velasco, P.; Wang, D.; Weber, A. Z.; Wang, L.-W.; Battaglia, V. S.; Yang, W.; Liu, G., Toward an ideal polymer binder design for high-capacity battery anodes. Journal of the American Chemical Society* ***2013,*** *135 (32), 12048-12056.*
11. *Zhao, H.; Wei, Y.; Qiao, R.; Zhu, C.; Zheng, Z.; Ling, M.; Jia, Z.; Bai, Y.; Fu, Y.; Lei, J.; Song, X.; Battaglia, V. S.; Yang, W.; Messersmith, P. B.; Liu, G., Conductive Polymer Binder for High-Tap-Density Nanosilicon Material for Lithium-Ion Battery Negative Electrode Application. Nano Letters* ***2015,*** *15 (12), 7927-7932.*
12. *Wu, H.; Yu, G.; Pan, L.; Liu, N.; McDowell, M. T.; Bao, Z.; Cui, Y., Stable Li-ion battery anodes by in-situ polymerization of conducting hydrogel to conformally coat silicon nanoparticles.* ***2013,*** *4, 1943.*
13. *Wegst, U. G. K.; Bai, H.; Saiz, E.; Tomsia, A. P.; Ritchie, R. O., Bioinspired structural materials. Nat Mater* ***2015,*** *14 (1), 23-36.*
14. *Lee, H.; Scherer, N. F.; Messersmith, P. B., Single-molecule mechanics of mussel adhesion. Proceedings of the National Academy of Sciences* ***2006,*** *103 (35), 12999-13003.*
15. *Maier, G. P.; Rapp, M. V.; Waite, J. H.; Israelachvili, J. N.; Butler, A., Adaptive synergy between catechol and lysine promotes wet adhesion by surface salt displacement. Science* ***2015,*** *349, 628-632.*
16. *Lee, H.; Lee, B. P.; Messersmith, P. B., A reversible wet/dry adhesive inspired by mussels and geckos. Nature* ***2007,*** *448 (7151), 338-341.*
17. *Liu, F.; Xie, L.-H.; Tang, C.; Liang, J.; Chen, Q.-Q.; Peng, B.; Wei, W.; Cao, Y.; Huang, W., Facile synthesis of spirocyclic aromatic hydrocarbon derivatives based on o-halobiaryl route and domino reaction for deep-blue organic semiconductors. Organic Letters* ***2009,*** *11 (17), 3850-3853.*
18. *Zhang, Q.; Divayana, Y.; Xiao, J.; Wang, Z.; Tiekink, E. R. T.; Doung, H. M.; Zhang, H.; Boey, F.;*

Sun, X. W.; Wudl, F., Synthesis, characterization, and bipolar transporting behavior of a new twisted polycyclic aromatic hydrocarbon: 1 ´,4 ´-diphenyl-naphtho-(2 ´.3 ´:1.2)-pyrene-6 ´-nitro-7 ´-methyl carboxylate. Chemistry – A European Journal ***2010,*** *16 (25), 7422-7426.*

19. *Stohr, J., NEXAFS Spectroscopy. Springer Science & Business Media: 1992.*
20. *Kovalenko, I.; Zdyrko, B.; Magasinski, A.; Hertzberg, B.; Milicev, Z.; Burtovyy, R.; Luzinov, I.; Yushin, G., A major constituent of brown algae for use in high-capacity Li-ion batteries. Science* ***2011,*** *334 (6052), 75-79.*
21. *Obrovac, M. N.; Chevrier, V. L., Alloy Negative Electrodes for Li-Ion Batteries. Chemical Reviews* ***2014,*** *114 (23), 11444-11502.*
22. *Obrovac, M. N.; Christensen, L., Structural Changes in Silicon Anodes during Lithium Insertion/Extraction. Electrochemical and Solid-State Letters* ***2004,*** *7 (5), A93-A96.*
23. *Zhao, H.; Wang, Z.; Lu, P.; Jiang, M.; Shi, F.; Song, X.; Zheng, Z.; Zhou, X.; Fu, Y.; Abdelbast, G.; Xiao, X.; Liu, Z.; Battaglia, V. S.; Zaghib, K.; Liu, G., Toward Practical Application of Functional Conductive Polymer Binder for a High-Energy Lithium-Ion Battery Design. Nano Letters* ***2014,*** *14 (11), 6704-6710.*